

Journal of Visualized Experiments

Live Imaging of the Mitochondrial Glutathione Redox State in Primary Neurons using a Ratiometric Indicator --Manuscript Draft--

Article Type:	Invited Methods Collection - JoVE Produced Video
Manuscript Number:	JoVE63073R2
Full Title:	Live Imaging of the Mitochondrial Glutathione Redox State in Primary Neurons using a Ratiometric Indicator
Corresponding Author:	Carlos Bas-Orth University of Heidelberg: Ruprecht Karls Universitat Heidelberg Heidelberg, BW GERMANY
Corresponding Author's Institution:	University of Heidelberg: Ruprecht Karls Universitat Heidelberg
Corresponding Author E-Mail:	bas-orth@uni-heidelberg.de
Order of Authors:	Athanasios Katsalifis Angela Maria Casaril Constanze Depp Carlos Bas-Orth
Additional Information:	
Question	Response
Please specify the section of the submitted manuscript.	Neuroscience
Please indicate whether this article will be Standard Access or Open Access.	Standard Access (\$1400)
Please indicate the city, state/province, and country where this article will be filmed . Please do not use abbreviations.	69120 Heidelberg, BW, Germany
Please confirm that you have read and agree to the terms and conditions of the author license agreement that applies below:	I agree to the Author License Agreement
Please confirm that you have read and agree to the terms and conditions of the video release that applies below:	I agree to the Video Release
Please provide any comments to the journal here.	

TITLE:

Live Imaging of the Mitochondrial Glutathione Redox State in Primary Neurons using a Ratiometric Indicator

AUTHORS AND AFFILIATIONS:

Athanasios Katsalifis¹ (ORCID: 0000-0003-3494-7617), Angela Maria Casaril¹ (ORCID: 0000-0003-4994-1891), Constanze Depp² (ORCID: 0000-0003-2868-6932), Carlos Bas-Orth¹ (ORCID: 0000-0002-6037-8350)

¹Department of Medical Cell Biology, Institute for Anatomy and Cell Biology, Heidelberg University, Im Neuenheimer Feld 307, D-69120 Heidelberg, Germany

²Department of Neurogenetics, Max-Planck-Institute for Experimental Medicine, Hermann-Rein-Straße 3, D-37075 Göttingen, Germany

Email addresses of co-authors:

Angela Maria Casaril	(angela.casaril@uni-heidelberg.de)
Athanasios Katsalifis	(bio2744@edu.biology.uoc.gr)
Constanze Depp	(depp@em.mpg.de)
Carlos Bas-Orth	(bas-orth@uni-heidelberg.de)

Corresponding author:

Carlos Bas-Orth (bas-orth@uni-heidelberg.de)

KEYWORDS:

Grx1-roGFP2, confocal microscopy, oxidative stress, hippocampal neurons, excitotoxicity, mitochondrial membrane potential

SUMMARY:

This article describes a protocol to determine differences in basal redox state and redox responses to acute perturbations in primary hippocampal and cortical neurons using confocal live microscopy. The protocol can be applied to other cell types and microscopes with minimal modifications.

ABSTRACT:

Mitochondrial redox homeostasis is important for neuronal viability and function. Although mitochondria contain several redox systems, the highly abundant thiol-disulfide redox buffer glutathione is considered a central player in antioxidant defenses. Therefore, measuring the mitochondrial glutathione redox potential provides useful information about mitochondrial redox status and oxidative stress. Glutaredoxin1-roGFP2 (Grx1-roGFP2) is a genetically encoded, green fluorescent protein (GFP)-based ratiometric indicator of the glutathione redox potential that has two redox-state-sensitive excitation peaks at 400 nm and 490 nm with a single emission peak at 510 nm. This article describes how to perform confocal live microscopy of mitochondria-targeted Grx1-roGFP2 in primary hippocampal and cortical neurons. It describes how to assess steady-state mitochondrial glutathione redox potential (e.g., to compare disease states or long-term

treatments) and how to measure redox changes upon acute treatments (using the excitotoxic drug *N*-methyl-D-aspartate (NMDA) as an example). In addition, the article presents co-imaging of Grx1-roGFP2 and the mitochondrial membrane potential indicator, tetramethylrhodamine, ethyl ester (TMRE), to demonstrate how Grx1-roGFP2 can be multiplexed with additional indicators for multiparametric analyses. This protocol provides a detailed description of how to (i) optimize confocal laser scanning microscope settings, (ii) apply drugs for stimulation followed by sensor calibration with diamide and dithiothreitol, and (iii) analyze data with ImageJ/FIJI.

INTRODUCTION:

Several important mitochondrial enzymes and signaling molecules are subject to thiol redox regulation¹. Moreover, mitochondria are a major cellular source of reactive oxygen species and are selectively vulnerable to oxidative damage². Accordingly, the mitochondrial redox potential directly affects bioenergetics, cell signaling, mitochondrial function, and ultimately cell viability^{3,4}. The mitochondrial matrix contains high amounts (1–15 mM) of the thiol-disulfide redox buffer glutathione (GSH) to maintain redox homeostasis and mount antioxidant defenses^{5,6}. GSH can be covalently attached to target proteins (S-glutathionylation) to control their redox status and activity and is used by a range of detoxifying enzymes that reduce oxidized proteins. Therefore, the mitochondrial glutathione redox potential is a highly informative parameter when studying mitochondrial function and pathophysiology.

roGFP2 is a variant of GFP that has been made redox-sensitive by the addition of two surface-exposed cysteines that form an artificial dithiol-disulfide pair^{7,8}. It has a single emission peak at ~510 nm and two excitation peaks at ~400 nm and 490 nm. Importantly, the relative amplitudes of the two excitation peaks depend on the redox state of roGFP2 (**Figure 1**), making this protein a ratiometric sensor. In the Grx1-roGFP2 sensor, human glutaredoxin-1 (Grx1) has been fused to the N-terminus of roGFP2^{9,10}. Covalent attachment of the Grx1 enzyme to roGFP2 affords two major improvements of the sensor: it makes the sensor response specific for the GSH/GSSG glutathione redox pair (**Figure 1**), and it speeds up equilibration between GSSG and roGFP2 by a factor of at least 100,000⁹. Therefore, Grx1-roGFP2 enables specific and dynamic imaging of the cellular glutathione redox potential.

Grx1-roGFP2 imaging can be performed on a wide range of microscopes, including widefield fluorescence microscopes, spinning disc confocal microscopes, and laser scanning confocal microscopes. Expression of the sensor in primary neurons can be achieved by various methods that include lipofection¹¹, DNA/calcium-phosphate coprecipitation¹², virus-mediated gene transfer, or use of transgenic animals as the cell source (**Figure 2**). Pseudotyped recombinant adeno-associated viruses (rAAV) containing a 1:1 ratio of AAV1 and AAV2 capsid proteins^{13,14} were used for the experiments in this article. With this vector, maximal sensor expression is typically reached 4–5 days after infection and stays stable for at least two weeks. We have successfully used Grx1-roGFP2 in primary hippocampal and cortical neurons from mice and rats.

In this article, rAAV-mediated expression of mitochondria-targeted Grx1-roGFP2 in primary rat hippocampal and cortical neurons is used to assess basal mitochondrial glutathione redox state and its acute perturbation. A protocol is provided for confocal live imaging with detailed

instructions on how to (i) optimize laser scanning confocal microscope settings, (ii) run a live imaging experiment, and (iii) analyze data with FIJI.

PROTOCOL:

All animal experiments conformed to national and institutional guidelines, including the Council Directive 2010/63/EU of the European Parliament, and had full Home Office ethical approval (University of Heidelberg Animal Welfare Office and Regierungspraesidium Karlsruhe, licenses T14/21 and T13/21). Primary hippocampal and cortical neurons were prepared from newborn mouse or rat pups according to standard procedures and were maintained for 12–14 days as previously described¹³.

1. Preparation of solutions

1.1. Stock solutions for imaging buffer

1.1.1. Prepare each stock solution according to **Table 1** and keep them at 4 °C. For long-term storage (>3 months), keep aliquots at -20 °C.

[Place **Table 1** here]

1.2. Stock solutions of drugs and dyes

1.2.1. Dissolve diamide (DA; used for calibration of maximal 405:488 ratio) in water to obtain a 0.5 M stock solution (e.g., 1 g in 11.615 mL of water). Aliquot and store at -20 °C.

1.2.2. Dissolve dithiothreitol (DTT; used for calibration of minimal 405:488 ratio) in water to obtain a 1 M stock solution (e.g., 5 g in 32.425 mL of water). Aliquot and store at -20 °C for a maximum of 3 months.

1.2.3. Dissolve N-methyl-D-aspartate (NMDA; used to induce excitotoxicity and mitochondrial oxidation) in water to obtain a 10 mM stock solution (e.g., 25 mg in 16.991 mL of water). Store the aliquots at -20 °C. For long-term storage (>6 months), keep the aliquots at -80 °C.

1.2.4. Tetramethylrhodamine ethyl ester perchlorate (TMRE; a small-molecule indicator of the mitochondrial membrane potential)

1.2.4.1. Dissolve TMRE powder in methanol to obtain a 20 mM stock (e.g., 25 mg in 2.427 mL of methanol).

1.2.4.2. Dilute the 20 mM stock 1:1,000 in methanol to obtain a 20 µM stock.

1.2.4.3. Aliquot the 20 mM and 20 µM stock solutions, seal with parafilm, and store protected from light at -20 °C.

NOTE: Both stock solutions are stable for several years. Use the 1,000x stock solution (20 μ M) for experiments.

1.3. Imaging buffer

1.3.1. Prepare 100 mL of imaging buffer by adding all components from **Table 2** to 80 mL of sterile water in a measuring cylinder. Bring the volume up to 100 mL with sterile water. Mix by carefully shaking the measuring cylinder until the solution appears homogeneous.

NOTE: It is recommended to use an osmometer to check the osmolarity of the buffer. It should be as close as possible to the growth medium of the cells. Here, this is 315 mOsmol/L. Increase or decrease the sucrose concentration as needed to match the osmolarity of the imaging buffer and growth medium.

1.3.2. Adjust the pH to 7.4. Make aliquots and keep them at 4 °C for up to two weeks. For long-term storage, keep the aliquots at -20 °C. Let the imaging buffer reach room temperature before use.

[Place **Table 2** here]

1.4. Solutions for stimulation and calibration

NOTE: Always prepare fresh stimulation solutions by adding stock solutions of indicated drugs to the imaging buffer just before the experiment. Solutions for stimulation and calibration will be added to the imaging chamber sequentially during an experiment (see sections 3–5). Depending on the type of experiment, different solutions are required to reach the same end concentration in the respective final volume in the imaging chamber.

1.4.1. Prepare 3x NMDA solution (90 μ M; final concentration in the chamber: 30 μ M) by adding 63 μ L of a 10 mM NMDA stock to 6.937 mL of imaging buffer. Add 500 μ L of the resulting solution to the chamber (final volume: 1.5 mL).

1.4.2. Prepare 2x DA solution for steps 3 and 4 (1 mM; final concentration in the chamber: 0.5 mM) by adding 14 μ L of a 0.5 M DA stock to 6.986 mL of imaging buffer. Add 1 mL to the chamber (final volume: 2 mL).

1.4.3. Prepare 4x DA solution for step 5 (2 mM; final concentration in the chamber: 0.5 mM) by adding 28 μ L of a 0.5 M DA stock to 6.972 mL of imaging buffer. Add 500 μ L to the chamber (final volume: 2 mL).

1.4.4. Prepare 1x DTT solution (5 mM; final concentration in the chamber: 5 mM) by adding 45 μ L of 1 M DTT stock to 8955 μ L of imaging buffer. Add 1 mL of this solution to the chamber after aspirating the imaging buffer (final volume: 1 mL).

2. Loading of cells with TMRE

NOTE: In this protocol, TMRE is used in non-quench mode¹⁵ at a final concentration of 20 nM. In general, the lowest possible concentration of TMRE that still provides sufficient signal intensity on the microscope of choice should be used. Due to uneven evaporation, the volume of medium in different wells can differ in long-term primary cultures. To ensure a consistent TMRE concentration in all wells, do not add TMRE directly to the wells. Instead, replace the medium in each well with the same amount of TMRE-containing medium. The protocol below is designed for primary neurons in 24-well plates containing ~1 mL of medium per well.

2.1. Working in a tissue culture laminar flow hood, collect 500 μ L of medium from each well into a single conical tube.

2.2. Per well, add 0.5 μ L of 20 μ M TMRE stock into the conical tube (e.g., 12 μ L for 24 wells).

2.3. Carefully aspirate the remaining medium from the first well and replace it with 500 μ L of TMRE-containing medium. Continue, well-by-well, with the remaining wells.

NOTE: Take care not to let the cells dry out and not to disturb the cells.

2.4. Return the cells to the incubator and wait for at least 60 min for dye equilibration.

NOTE: Loading time can be extended to several hours without adverse effects.

2.5. To ensure consistent TMRE concentrations and equilibration throughout the imaging experiment, make sure to include a final concentration of 20 nM TMRE in the imaging buffer and all stimulation solutions.

3. Optimization of scanning confocal microscope settings

NOTE: This step aims to find the best compromise between image quality and cell viability during live imaging. This section describes the optimization of settings for roGFP imaging. If multiparametric imaging is performed, similar optimization, including checking for a stable baseline without signs of bleaching or phototoxicity, needs to be performed for the additional indicators. mito-Grx1-roGFP2 imaging can be performed at room temperature or 35–37 °C on a heated stage. The sensor will work in both cases; however, the kinetics of signaling cascades and enzyme reactions inside the cells will naturally differ based on temperature.

3.1. Start the confocal microscope and load standard settings for GFP imaging (**488 nm excitation, 505–550 nm emission**).

3.2. Set the **detector to 12 bits or 16 bits**.

NOTE: Usually, 8 bits are not sufficient for quantitative imaging.

3.3. Activate the **sequential scan** mode and add **second sequence/track (405 nm excitation, 505–550 nm emission)**.

3.4. For both channels, select a **pseudocolor lookup table** that indicates over- and under-exposed pixels (e.g., **GLOW OU**).

3.5. Select an objective that is suitable for the object of interest.

NOTE: 10x–40x are suitable for single-cell analysis, 63x–100x are suitable for single-mitochondrion analysis.

3.6. Mount a coverslip with cells into the imaging chamber, add 1 mL of imaging buffer, and place the chamber on the microscope.

3.7. Use the eyepiece and transmitted light to focus the cells.

NOTE: Do not use epifluorescence light to locate and focus cells. Even at low power, this will adversely affect the cells.

3.8. **Record images with different pixel formats.** Based on these images, select the lowest pixel number that gives an acceptable resolution of the structure of interest.

NOTE: Typically, 512 x 512 pixels work well for single-cell imaging with 20x and 40x objectives, and 1024 x 1024 or 2048 x 2048 pixels typically work well for single-mitochondrion imaging with a 63x objective.

3.9. **Record images with different pinhole sizes.** Based on these images, select the largest pinhole size that gives an acceptable resolution of the structure of interest.

NOTE: Typically, 3–7 airy units typically work well.

3.10. **Record images with different laser intensities.**

3.10.1. **Adjust the detector gain and threshold accordingly.** Based on these images, select the lowest laser intensity that gives acceptable signal intensity and signal-to-background ratio.

3.10.1.1. To determine the signal-to-background ratio, measure the signal intensity in a region of interest (ROI) that contains cells or mitochondria (ROI1) and in an ROI without cells or mitochondria (ROI2). Then, divide the intensity of ROI1 by the intensity of ROI2.

NOTE: Aim for a signal-to-background ratio of >3 and signal intensities of individual ROIs of 200–1,000 for 405 nm excitation with 1–3% laser power and intensities of individual ROIs of 300–1,500

for 488 nm excitation with 1% laser power.

3.11. **Record images with different scan speeds and number of frame averages.** Record 4–5 images for each combination of settings. Based on these image series, select the highest speed and lowest average settings that give acceptable image noise and image-to-image variability.

NOTE: A scan speed of 600 Hz and 1–2 frames for averaging work well in most cases.

3.12. Using a new coverslip, record a time-lapse series with the optimized settings.

NOTE: The duration and image interval of the series should resemble those of the planned experiments.

3.13. At the end of the time-lapse series, add 1 mL of 2x DA solution to the recording chamber. Image for additional 2 min.

3.14. Aspirate the imaging buffer using a peristaltic pump or handheld pipette. Add 1 mL of 1x DTT solution. Image for additional 5 min.

3.15. Analyze the time-lapse experiment (see section 5).

3.15.1. Verify that none of the two channels gets over- or under-exposed during DA- and DTT-treatment with the optimized settings.

3.15.2. Ensure that none of the two channels shows considerable bleaching during the time-lapse recording; aim for <2% loss of intensity between the first and last images.

3.15.3. Verify that the 405:488 ratio does not change considerably during imaging.

3.16. Repeat the whole procedure in an iterative manner, using several coverslips, until settings that consistently provide acceptable results have been defined.

4. Assessment of basal redox status

4.1. Start the microscope and load the optimized settings from section 3.

4.2. Set **frame average** to **3–5**.

4.3. Mount a coverslip with cells into the imaging chamber, add 1 mL of imaging buffer, and place the chamber on the microscope.

4.4. Use the eyepiece and transmitted light to focus the cells.

NOTE: Do not use epifluorescence light to locate and focus cells. Even at low power, this will

adversely affect the cells.

4.5. Switch to **scanning** mode and use the **488 nm channel** in **live view** to focus and locate cells for imaging.

4.6. Use the **multipoint function** to select 3–5 fields of view on the coverslip.

4.7. Record a baseline image.

4.8. Add 1 mL of 2x DA solution to the chamber.

4.9. After 1, 2, and 3 min, use **live view** to confirm/adjust the focus and record an image.

NOTE: Cells are typically fully oxidized after 2 min.

4.10. Replace the buffer in the imaging chamber with 1 mL of 1x DTT solution.

4.11. After 3 and 5 min, use **live view** to confirm/adjust the focus and record an image.

NOTE: Cells are typically fully reduced after 4–5 min.

5. Live imaging of acute treatments

NOTE: The protocol below describes imaging of the mitochondrial redox response to NMDA treatment. Image intervals and duration of the experiment might need to be adjusted for other treatments.

5.1. Start the microscope and load the optimized settings from section 3.

5.2. Set the **time-lapse interval to 30 s** and **duration to 25 min**.

5.3. Mount a coverslip with cells into the imaging chamber, add 1 mL of imaging buffer, and **place the chamber on the microscope**.

NOTE: To avoid thermal focus drift, leave the cells on the microscope stage for 10–15 min before starting time-lapse imaging.

5.4. Use the eyepiece and transmitted light to focus the cells.

NOTE: Do not use epifluorescence light to locate and focus cells. Even at low power, this will adversely affect the cells.

5.5. Switch to the **scanning mode** and use the **488 nm channel** in **live view** to focus and locate cells for imaging.

5.6. Optional: To increase the number of recorded cells per run, use the **multipoint function** to image 2–3 fields of view per coverslip.

5.7. Start the time-lapse acquisition and record 5 images as 2 min baseline recording.

5.8. Add 500 μ L of 3x NMDA solution to the chamber (final concentration 30 μ M) and record additional 20 images as a 10 min NMDA response.

NOTE: Neurons are very sensitive to changes in osmolarity. Therefore, make sure to minimize evaporation of the imaging buffer. For longer treatments, the imaging chamber should be covered with a lid.

5.9. Add 500 μ L of 4x DA solution to the chamber and record 6 more images (3 min maximum calibration).

5.10. Aspirate the buffer from the imaging chamber and replace it with 1 mL of 1x DTT solution. Record 10 more images (5 min minimum calibration).

5.11. End the recording and save the image series.

6. Data analysis

6.1. Data import and image preprocessing in FIJI

6.1.1. Use the **Bio-Formats Importer** to open a group of images from step 4 or an image file from step 5. Click on **Plugins | Bio-Formats | Bio-Formats Importer**. In the dialog box, use **View stack with: Hyperstack**, set **Color mode: default**, select **Autoscale**, and do not split into separate windows.

NOTE: **Autoscale** optimizes the display of the data on the computer screen. It does not change pixel intensities.

6.1.2. If individual images from step 4 were opened, click on **Image | Stacks | Tools | Concatenate** to merge them into a single-image stack.

6.1.3. If there is XY-drift during the image series, click on **Plugins | StackReg** to register the images. In the dialog box, select **Rigid Body** or **Translation**.

6.1.4. Change the image format to 32 bit by clicking on **Image | Type | 32-bit**.

6.1.5. Split the color channels into separate windows by clicking on **Image | Color | Split Channels**.

6.1.6. Select **channel 1 (405 nm)** and adjust the threshold to select the mitochondria for analysis by clicking on **Image | Adjust | Threshold**. In the dialog box, select **Default, Red, Dark background**, and **Stack histogram** and wait for the selected pixels to appear red. Click **Apply**. Select **Set Background Pixels to NaN** and **Process all images**.

NOTE: To avoid potential observer bias, automated threshold determination should be used. FIJI offers several automated methods (such as Default, Huang, Intermodes, Otsu) that can be selected from a dropdown menu in the threshold dialog box. Typically, the Default method gives a good result. It is recommended to compare several methods during the first analysis to find the best thresholding method for the given set of images. Once a method has been chosen, it needs to be applied to all images.

6.1.7. Repeat step 6.1.6 for **channel 2 (488 nm)**.

6.1.8. Create a ratio image to visualize the 405:488 nm ratio by clicking on **Process | Image calculator**. In the dialog box, select **Image 1: channel 1, Operation: Divide, Image 2: channel 2, Create new window, Process all images**.

6.1.9. Change the **lookup table** of the ratio image to **pseudocolor**. For example, to change to **Fire**, click on **Image | Lookup Tables | Fire**.

6.2. Image analysis

6.2.1. On the ratio image, draw ROIs around individual cells or mitochondria. After drawing each ROI, add it to the **ROI Manager**. **Analyze | Tools | ROI Manager | Add**. (keyboard shortcut: 'T') Select **Show All**.

NOTE: Because background pixels have been set to 'not a number' (NaN) in steps 6.1.6 and 6.1.7, they will not affect the result of the measurement. Therefore, it is acceptable to include some background pixels in the ROI.

6.2.2. Measure the 405:488 ratios of individual cells by clicking on **ROI Manager | ctrl+A to select all ROIs | More | Multi Measure**. In the dialog box, select **Measure all slices** and **One row per slice**.

6.2.3. Export the measurements to spreadsheet software.

6.2.4. Select the **405 nm image**. Measure the intensities of all ROIs as in step 6.2.2. using the ROIs that are stored in the ROI manager.

6.2.5. Export the measurements to spreadsheet software.

6.2.6. Select the **488 nm image**. Measure intensities of all ROIs as in step 6.2.2. using the ROIs that are stored in the ROI manager.

6.2.7. Export the measurements to spreadsheet software.

6.2.8. Save ROIs for future reference by clicking on **ROI Manager | ctrl+A to select all ROIs | More | Save.**

6.2.9. Recommended: Generate intensity vs. time plots of the 405 and 488 nm traces. Verify that there is no marked bleaching in either of the channels (signal intensity at the end of the imaging series should be $\geq 98\%$ of the first image) and that the two traces move into opposite directions during sensor responses (e.g., the 405 nm trace should increase during oxidation while the 488 nm trace should decrease).

6.3. Data normalization

6.3.1. For each ROI from the ratio image, determine the maximum value during DA treatment (R_{\max}) and the minimum value during DTT treatment (R_{\min}).

6.3.2. Calculate the normalized ratio as follows:

$$R = (R - R_{\min}) / (R_{\max} - R_{\min})$$

NOTE: This will set the maximum ratio to 1.0 and the minimum ratio to 0.

6.4. Analysis of mitochondrial morphology

6.4.1. To obtain measurements of mitochondrial morphology in parallel to roGFP intensities in step 6.2.6, go to **Analyze | Set Measurements** and check **Shape descriptors** and **Fit ellipse**.

NOTE: In addition to mean intensity, the measurements in the **results** window will include the length of the major axis (**Major**), the length of the minor axis (**Minor**), the aspect ratio (**AR**; major axis divided by minor axis; round mitochondria have an AR ~ 1 , elongated mitochondria have a greater AR), as well as measurements of circularity (**Circ.**) and roundness (**Round**).

REPRESENTATIVE RESULTS

Quantification of differences in steady-state mitochondrial redox state after growth factor withdrawal

To demonstrate the quantification of steady-state differences in mitochondrial redox state, primary neurons grown in standard medium were compared to neurons cultured without growth factors for 48 h before imaging. Growth factor withdrawal results in apoptotic neuronal cell death after 72 h¹⁶. Cells were imaged after 48 h to test if this is preceded by changes in mitochondrial redox state. Primary rat cortical neurons grown on poly-L-ornithine-coated coverslips were infected with rAAV-mito-Grx1-roGFP2 on days *in vitro* 6 (DIV6) and were imaged on DIV12. Live imaging was performed at room temperature according to section 4 of this protocol on an inverted laser scanning confocal microscope equipped with a 40x/1.10 water immersion

objective. Confocal settings were pinhole 7 airy units, pixel size 568.7 nm (512 x 512 pixels), scan speed 600 Hz, laser power 405 nm 3%, laser power 488 nm 1%, emission bandwidth 505–550 nm, and frame average 4. There was no major difference between the raw 405:488 nm ratios of the two conditions (**Figure 3B**). After data normalization, a subset of cells with an increased 405:488 nm ratio was detectable in the growth factor withdrawal group (**Figure 3C**). This indicates that mitochondrial redox changes might precede neuronal cell death, and it underscores the relevance of max/min data normalization for the comparison of basal redox states between groups.

Dynamic changes in mitochondrial redox state upon treatment of neurons with NMDA

The NMDA-type glutamate receptor (NMDAR) plays a central role in neuronal plasticity but can also mediate neuronal damage and cell death. Pathological activation of the NMDAR leads to several adverse effects on mitochondria that include matrix calcium overload, mitochondrial oxidation and fragmentation, and mitochondrial permeability transition. In a previous study, the above-described protocol was used to investigate a causal relationship between NMDA-induced mitochondrial calcium overload and mitochondrial oxidation¹³. Primary rat hippocampal neurons grown on poly-D-lysine/laminin-coated coverslips were infected with rAAV-mito-Grx1-roGFP2 on DIV4 and imaged on DIV12. Live imaging was performed at 37 °C on an inverted spinning disc confocal microscope equipped with a 20x/0.75 multi immersion objective (water immersion was used) and an on-stage incubation system. Mito-Grx1-roGFP2 was sequentially excited every 20 s using the 405 nm and 488 nm laser lines, and emission was collected with a 527/55 nm emission filter for both excitation wavelengths. Treatment of neurons with 30 μM NMDA caused oxidation of mitochondria within a few minutes (**Figure 4A,B**). Notably, NMDA-induced mitochondrial acidosis caused significant quenching of roGFP2 fluorescence, in line with its well-known pH-sensitivity⁸. To confirm that this pH-dependent quenching did not affect the 405:488 ratio⁹, mitochondria were fully oxidized by DA before the addition of NMDA in a control experiment. Pretreatment with DA precludes any further oxidation of mitochondria by NMDA and, accordingly, the 405:488 ratio did not change in this experiment despite a considerable quenching of roGFP2 fluorescence intensity (**Figure 4C**).

Multiparametric analysis of NMDA-induced changes of dendritic mitochondria

To assess the temporal sequence of NMDA-induced changes in mitochondrial morphology, membrane potential, and redox state, parallel imaging of TMRE- and mito-Grx1-roGFP2 fluorescence was performed at high spatial and temporal resolution. Primary rat cortical neurons grown on poly-L-ornithine-coated coverslips were infected with rAAV-mito-Grx1-roGFP2 on DIV6 and imaged on DIV12. Live imaging was performed at room temperature on an inverted confocal laser scanning microscope using a 63x/1.40 oil immersion objective, a scan speed of 600 Hz, a pixel size of 90.2 nm (1024 x 1024 pixels at 2x scan zoom), a pinhole size of 3 airy units, and a frame average of 2. Every 30 s, three images were recorded in sequential mode: 405 nm excitation/505–550 nm emission; 488 nm excitation/505–550 nm emission; 552 nm excitation/560–600 nm emission. Treatment of neurons with 60 μM NMDA resulted in a loss of TMRE signal and an increase in the 405:488 nm roGFP ratio, followed by some delayed rounding up of mitochondria (**Figure 5**).

FIGURE AND TABLE LEGENDS:

Figure 1: Schematic representation of Grx1-roGFP2 function and roGFP2 excitation spectra. (A) Oxidative stress and the action of antioxidant defense systems oxidize the cellular glutathione pool. Grx1 in the Grx1-roGFP2 fusion protein promotes the rapid equilibration of the roGFP2 redox state with the redox state of the glutathione pool. The redox status of the roGFP2 pool can be assessed by monitoring the ratio of GFP-fluorescence emission at 510 nm after excitation at 405 nm and 488 nm. Reduced species are shown in blue; oxidized species are shown in red. **(B)** Excitation spectra of fully reduced (blue) and oxidized (red) roGFP2. Upon oxidation of roGFP2, fluorescence emission at 400 nm excitation increases, whereas emission at 490 nm excitation decreases. This figure has been modified from a previous publication¹³. Excitation spectra in **B** were drawn based on **Figure 1B** from ⁸. Dotted lines in **B** indicate the wavelengths of commonly used 405 nm and 488 nm laser lines. Abbreviations: GSH = glutathione; GSSG = oxidized glutathione; Grx = glutaredoxin; roGFP = redox-sensitive green fluorescent protein variant.

Figure 2: Workflow of the method. Expression of the excitation-ratiometric redox-sensitive fluorescent protein roGFP2 in neurons can be achieved through several methods that include transfection, lipofection, viral gene transfer, and transgenic animals. The sensor can be used to study the neuronal redox state in cultured primary neurons, *ex vivo* tissue explants, and intact animals. roGFP2 imaging can be performed on a variety of microscopes that include widefield fluorescent microscopes, confocal microscopes, and 2-photon microscopes. Analysis of roGFP2 imaging data can be performed with the freely available software ImageJ/FIJI. Abbreviation: roGFP = redox-sensitive green fluorescent protein variant.

Figure 3: Growth factor withdrawal causes oxidation of neuronal mitochondria. (A) Representative 405:488 nm ratio images of neurons cultured in the presence (+ GF) or absence (-GF) of growth factors for 48 h before imaging. Color-coded scales represent non-normalized 405:488 nm ratios (lower ratios correspond to a reduced state; higher ratios correspond to an oxidized state). Scale bars = 50 μ m. **(B)** Quantification of the 405:488 nm ratio in individual neurons. **(C)** Max/min calibrated 405:488 nm ratio of individual neurons. Round symbols represent single cells; bar represents mean. N = 40–44 cells from 3 coverslips from one preparation. Abbreviation: GF = growth factor.

Figure 4: NMDA-induced oxidation of neuronal mitochondria. (A) Representative 405:488 nm ratio images before and after treatment with 30 μ M NMDA and after max/min calibration with DA and DTT. At this magnification, roGFP signal is mostly detected in the soma and proximal dendrites. The color-coded scale represents non-normalized 405:488 nm ratios (lower ratios correspond to a reduced state; higher ratios correspond to an oxidized state). Scale bars = 50 μ m. **(B)** Quantification of the imaging run shown in **A**. NMDA induces a rapid and sustained mitochondrial oxidation that can be calibrated using DA and DTT. **(C)** NMDA-induced mitochondrial acidosis causes a drop of GFP fluorescence upon both 405 nm and 488 nm excitation (upper panel). To isolate the pH-driven effect and confirm that the 405:488 nm ratio is pH-insensitive, neurons were first maximally oxidized using DA and subsequently challenged with NMDA in the presence of DA (lower panel). Under these conditions, NMDA still causes mitochondrial acidosis but no further mitochondrial oxidation. Accordingly, although both the 405 nm and 488 nm trace show a pH-driven drop in fluorescence intensity, the 405:488 nm ratio

remains stable. This figure is modified from ¹³. Abbreviations: GFP = green fluorescent protein; roGFP = redox-sensitive green fluorescent protein variant; NMDA = N-methyl-D-aspartate; DA = diamide; DTT = dithiothreitol.

Figure 5: NMDA-induced changes in membrane potential, redox state, and morphology of dendritic mitochondria. (A) Three high-magnification images from a time-lapse experiment, acquired at t = 1, 4, and 9 min, showing dendritic and axonal mitochondria. Colorization represents TMRE intensity (see calibration bar). (B) 405:488 nm roGFP ratio images from the same time-lapse experiment as in (A) at t = 1, 4, and 9 min. Note that due to limited AAV infection efficiency, only a subset of neurons expresses mito-Grx1-roGFP2, and therefore, not all TMRE-positive mitochondria are roGFP-positive. The color-coded calibration bar represents non-normalized 405:488 nm ratios (lower ratios correspond to a reduced state; higher ratios correspond to an oxidized state). (C) Quantification of TMRE intensity, roGFP 405:488 nm ratio, and roundness of a single mitochondrion (indicated by arrows in A, B). After 1 min of baseline recording, 60 μ M NMDA was added to the bath solution. Scale bars = 5 μ m. The y-axis in C depicts the 405:488 nm roGFP ratio relative to baseline T₀ (green dashed line), the TMRE fluorescence intensity relative to baseline T₀ (red dotted line), and the FIJI/ImageJ shape descriptor “roundness” (black solid line). Abbreviations: GFP = roGFP = redox-sensitive green fluorescent protein variant; mito-Grx1-roGFP2 = Glutaredoxin-1 fused to N-terminus of roGFP; AAV = adeno-associated virus; TMRE = tetramethylrhodamine, ethyl ester; NMDA = N-methyl-D-aspartate.

Table 1: Stock solutions for imaging buffer.

Table 2: Composition of imaging buffer. The indicated volumes are used for the preparation of 100 mL of imaging buffer.

DISCUSSION

Quantitative and dynamic measurements of the mitochondrial redox state provide important information about mitochondrial and cellular physiology. Several fluorogenic chemical probes are available that detect reactive oxygen species, “redox stress,” or “oxidative stress.” However, the latter terms are not well-defined and often lack specificity^{9,17,18}. Compared to chemical dyes, Grx1-roGFP2 offers several advantages^{9,19}: (i) as an excitation-ratiometric sensor, it provides inherent normalization for sensor expression level, absolute fluorescence intensity, and cell or organelle density; (ii) as a genetically encoded probe, it can be targeted to organelles or specific subcellular compartments such as presynaptic terminals or postsynaptic dendritic spines; (iii) genetic expression of the sensor obviates the need for dye loading, which in the case of chemical dyes can be stressful for primary neurons; (iv) in contrast to general redox-sensitive chemical dyes, Grx1-roGFP2 is highly specific for the glutathione redox potential; (v) oxidation and reduction of the sensor are reversible, enabling the measurement of transient redox changes; (vi) in contrast to chemical dyes that allow for the detection of relative changes only, Grx1-roGFP2 fluorescence ratios can be calibrated to determine absolute redox potentials in mV⁹.

This protocol describes dynamic measurements of the mitochondrial glutathione redox potential in primary neurons. Analysis of mitochondria within intact cells has several advantages¹⁵.

Compared to the study of isolated mitochondria, mitochondria within cells retain physiologically relevant contacts with other organelles (e.g., endoplasmic reticulum–mitochondria contacts, mitochondria–lysosome contacts) and are exposed to cellular concentrations of signaling molecules and metabolites. Compared to the study of intact animals, primary neurons provide better accessibility for genetic and pharmacological manipulations and microscopy. However, for certain questions, analysis of isolated mitochondria will be better suited as this allows precise control over delivered substrates and inhibitors. Notably, mito-Grx1-roGFP2 can also be used in isolated mitochondria²⁰. To study neuronal mitochondria within intact tissues or animals, transgenic fly and mouse lines are available that express mito-Grx1-roGFP2 in the nervous system²¹⁻²³. Notably, the excitation spectrum of roGFP2 is amenable to two-photon excitation, enabling *ex vivo* and *in vivo* two-photon imaging in tissue explants and intact animals, respectively^{23,24}. Spectral variants of thiol redox-sensitive fluorescent proteins are also available such as yellow rxYFP-Grx1p²⁵ and red Grx1-roCherry²⁶. These provide additional flexibility for multiplexing and, in principle, enable the simultaneous measurement of redox-responses in different cell types or cellular compartments.

As described in the protocol, the 405:488 nm ratio can be calibrated by measuring maximal and minimal fluorescence ratios after the application of DA and DTT, respectively. This normalization is not essential because the sensor provides a certain degree of inherent normalization due to its ratiometric nature. However, we recommend performing max/min calibration after each imaging run, mostly for two reasons. First, it ensures that sensor responses were not saturated during the experiment. Second, the absolute 405:488 nm ratio is an arbitrary number that depends on the microscope settings of both channels. Even when keeping the same settings, one cannot be sure that laser power and detector performance will stay the same between experiments, especially when these are several weeks apart. One workaround would be to set the average baseline ratio of control cells to 1.0 within each experiment. This allows for relative quantification of treatment-induced redox perturbations in a given experiment but limits the comparability of different experiments. Especially when comparing the basal redox state of cells from different experiments or cell types, it is important to obtain max/min calibrated absolute quantification. Occasionally, the 405:488 nm ratio does not fall below the baseline ratio after DTT treatment, especially if the mitochondria were already in a relatively reduced state at baseline. This typically is a sign of sensor bleaching during prolonged time-lapse experiments. In this case, repeat the experiment with microscope settings that cause less light exposure.

It is paramount to use microscope settings that do not cause bleaching of the sensor or phototoxicity-induced oxidation of mitochondria. Make sure to take sufficient time for protocol optimization before starting actual experiments. Once acceptable settings have been defined, they can be used in subsequent experiments with minimal adjustments. Therefore, kinetics and amplitudes of sensor responses may vary depending on the chosen temperature. The choice of temperature is up to the user, depending on the specific needs of the experiment.

Finally, we would like to point out two limitations of the sensor. First, the intensity of emitted light is considerably lower with excitation at 405 nm than with excitation at 488 nm, often resulting in rather noisy 405 nm images. Higher laser power is needed to improve the signal to

noise in the 405 nm channel. However, excitation at 405 nm is typically more phototoxic and generates more autofluorescence than excitation at 488 nm, limiting the permissible 405 nm laser intensity. For example, in this study, weak roGFP fluorescence combined with considerable 405 nm-excited tissue autofluorescence prevented the acquisition of robust data from mito-Grx1-roGFP2-expressing ganglion cells in live retina flatmounts (Depp and Bas-Orth, unpublished observation). Second, although the 405:488 nm ratio is insensitive to pH changes within a physiological range around pH 5.5 to pH 8.5 (**Figure 4**)⁹, pH-dependent quenching of roGFP2 emission can cause the typically weak 405 nm signal to drop below the detection limit of the microscope, preventing the acquisition of quantifiable ratio images. For example, this was the case during NMDA-induced acidosis in the neuronal cytosol¹³.

ACKNOWLEDGMENTS:

This work was supported by the Deutsche Forschungsgemeinschaft (BA 3679/5-1; FOR 2289: BA 3679/4-2). A.K. is supported by an ERASMUS+ fellowship. We thank Iris Bünzli-Ehret, Rita Rosner, and Andrea Schlicksupp for the preparation of primary neurons. We thank Dr. Tobias Dick for providing pLPCX-mito-Grx1-roGFP2. Experiments shown in **Figure 4** were performed at the Nikon Imaging Center, University of Heidelberg. **Figure 2** was prepared with BioRender.com.

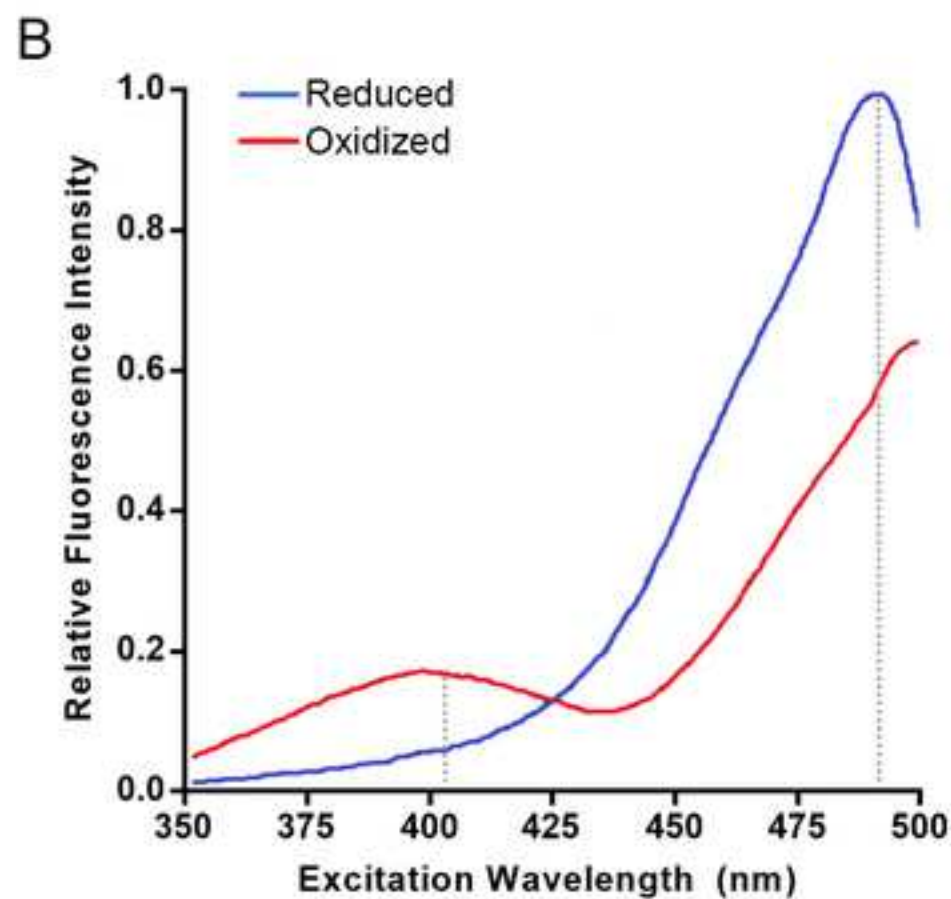
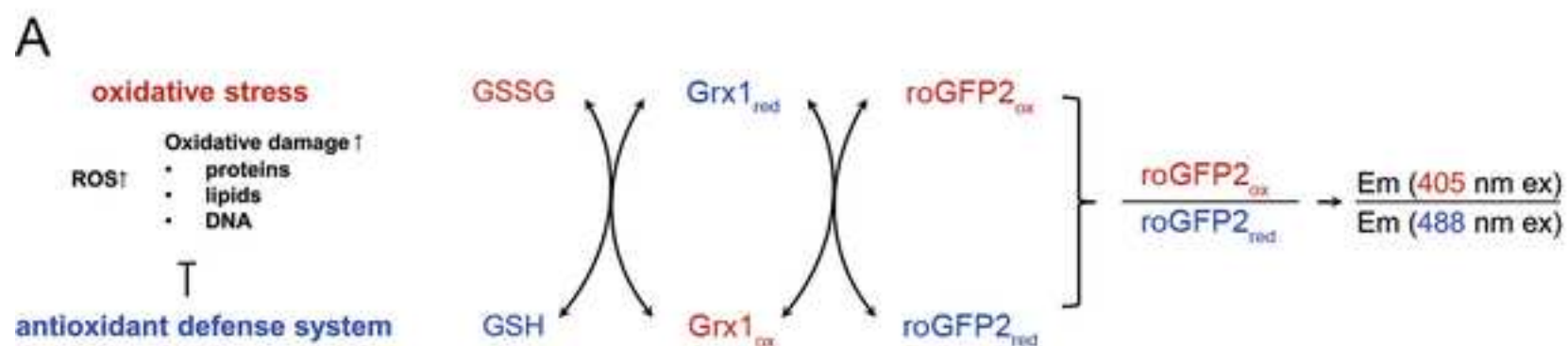
DISCLOSURES:

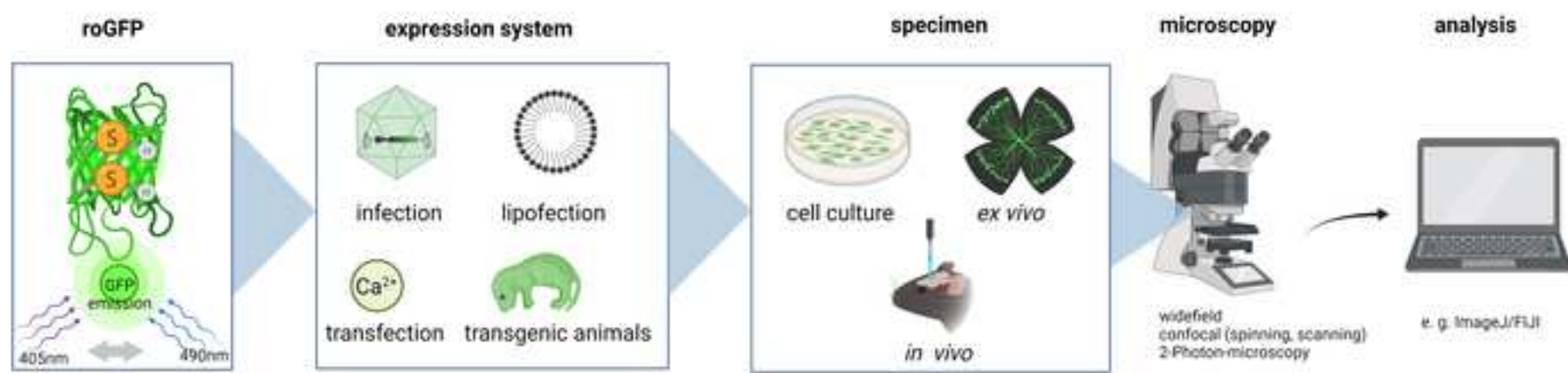
The authors declare that they have no conflict of interest.

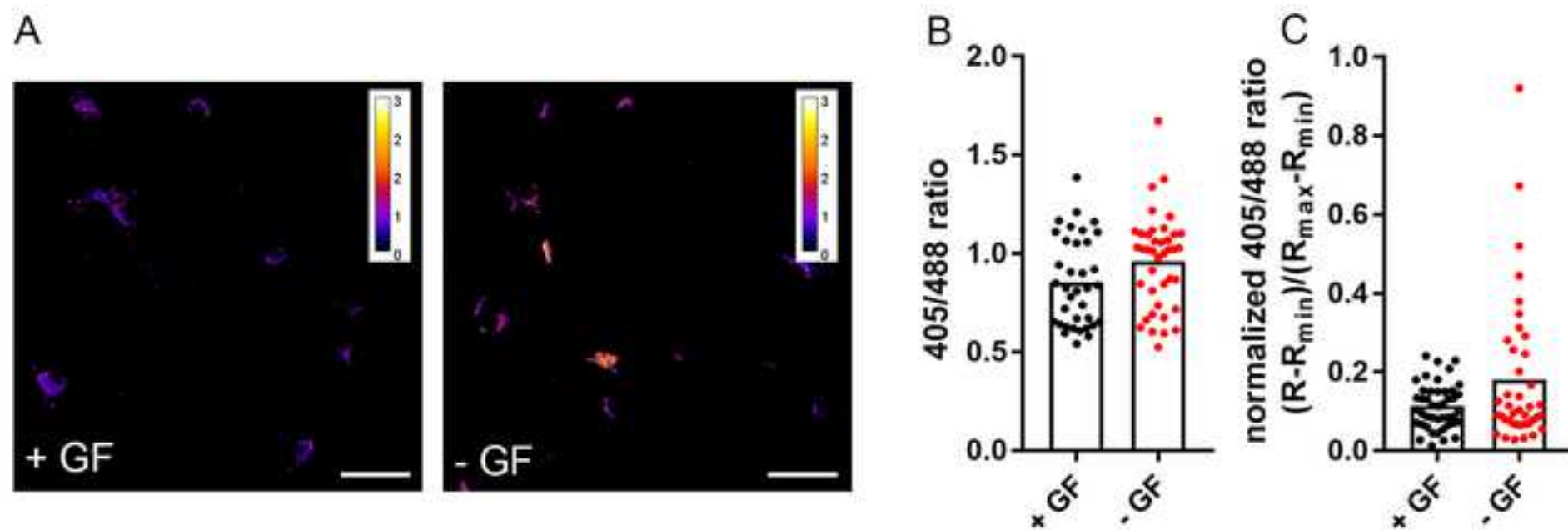
REFERENCES:

- 1 Roede, J. R., Go, Y. M., Jones, D. P. Redox equivalents and mitochondrial bioenergetics. *Methods in Molecular Biology*. **810**, 249–280 (2012).
- 2 Turrens, J. F. Mitochondrial formation of reactive oxygen species. *Journal of Physiology*. **552** (Pt 2), 335–344 (2003).
- 3 Lin, M. T., Beal, M. F. Mitochondrial dysfunction and oxidative stress in neurodegenerative diseases. *Nature*. **443** (7113), 787–795 (2006).
- 4 Manfredi, G., Beal, M. F. The role of mitochondria in the pathogenesis of neurodegenerative diseases. *Brain Pathology*. **10** (3), 462–472 (2000).
- 5 Mari, M., Morales, A., Colell, A., Garcia-Ruiz, C., Fernandez-Checa, J. C. Mitochondrial glutathione, a key survival antioxidant. *Antioxidants & Redox Signaling*. **11** (11), 2685–2700 (2009).
- 6 Murphy, M. P. Mitochondrial thiols in antioxidant protection and redox signaling: distinct roles for glutathionylation and other thiol modifications. *Antioxidants & Redox Signaling*. **16** (6), 476–495 (2012).
- 7 Dooley, C. T. *et al.* Imaging dynamic redox changes in mammalian cells with green fluorescent protein indicators. *Journal of Biological Chemistry*. **279** (21), 22284–22293 (2004).
- 8 Hanson, G. T. *et al.* Investigating mitochondrial redox potential with redox-sensitive green fluorescent protein indicators. *Journal of Biological Chemistry*. **279** (13), 13044–13053 (2004).
- 9 Gutscher, M. *et al.* Real-time imaging of the intracellular glutathione redox potential. *Nature Methods*. **5** (6), 553–559 (2008).
- 10 Morgan, B., Sobotta, M. C., Dick, T. P. Measuring E(GSH) and H₂O₂ with roGFP2-based redox probes. *Free Radical Biology & Medicine*. **51** (11), 1943–1951 (2011).

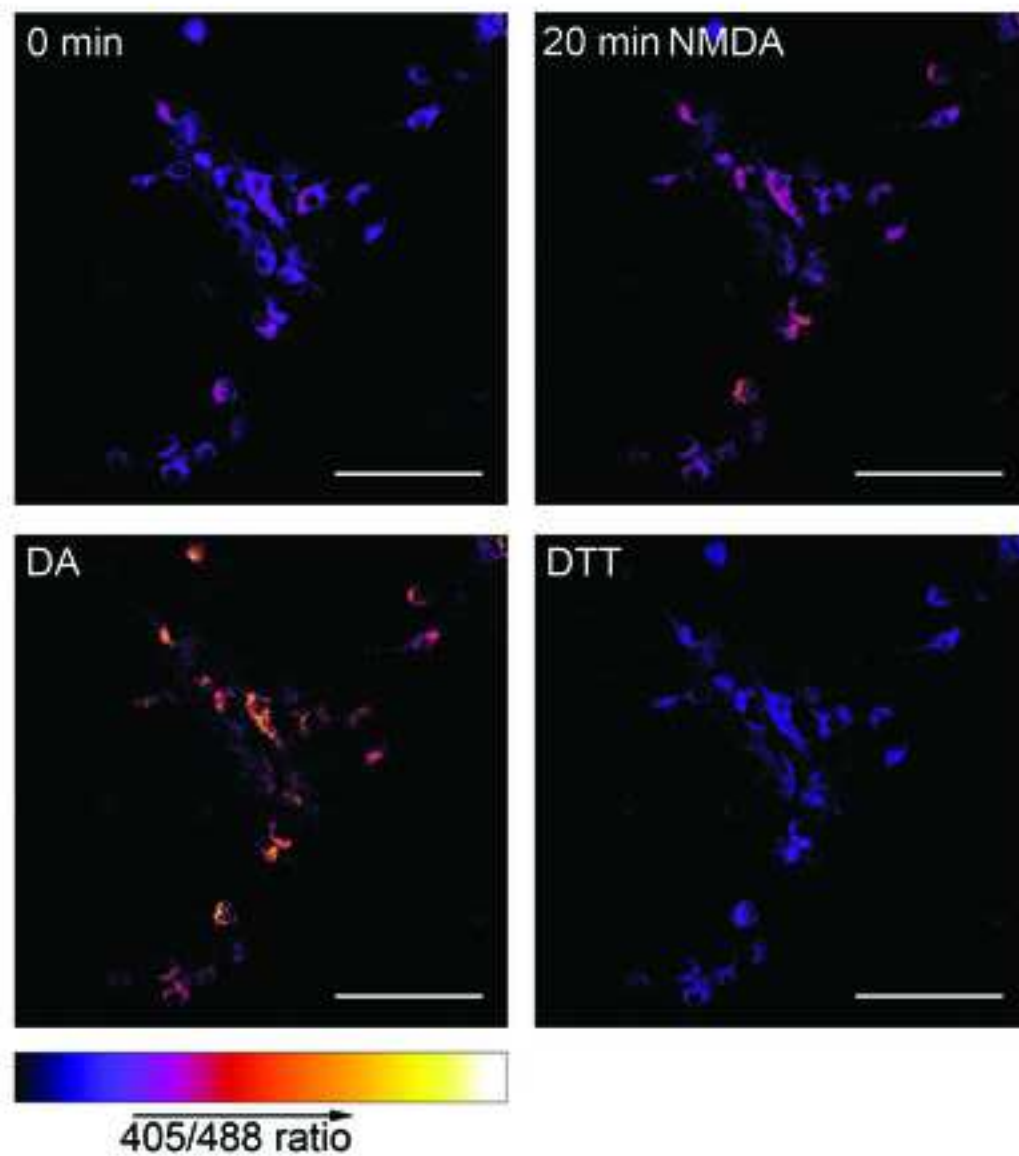
- 11 Marwick, K. F. M., Hardingham, G. E. Transfection in primary cultured neuronal cells. *Methods in Molecular Biology*. **1677**, 137–144 (2017).
- 12 Kohrmann, M. *et al.* Fast, convenient, and effective method to transiently transfect primary hippocampal neurons. *Journal of Neuroscience Research*. **58** (6), 831–835 (1999).
- 13 Depp, C., Bas-Orth, C., Schroeder, L., Hellwig, A., Bading, H. Synaptic activity protects neurons against calcium-mediated oxidation and contraction of mitochondria during excitotoxicity. *Antioxidants & Redox Signaling*. **29** (12), 1109–1124 (2018).
- 14 Hauck, B., Chen, L., Xiao, W. Generation and characterization of chimeric recombinant AAV vectors. *Molecular Therapy*. **7** (3), 419–425 (2003).
- 15 Brand, M. D., Nicholls, D. G. Assessing mitochondrial dysfunction in cells. *Biochemical Journal*. **435** (2), 297–312 (2011).
- 16 Zhang, S. J. *et al.* Nuclear calcium signaling controls expression of a large gene pool: identification of a gene program for acquired neuroprotection induced by synaptic activity. *PLoS Genetics*. **5** (8), e1000604 (2009).
- 17 Winterbourn, C. C. The challenges of using fluorescent probes to detect and quantify specific reactive oxygen species in living cells. *Biochimica et Biophysica Acta*. **1840** (2), 730–738 (2014).
- 18 Sies, H. Oxidative stress: a concept in redox biology and medicine. *Redox Biology*. **4**, 180–183 (2015).
- 19 Lukyanov, K. A., Belousov, V. V. Genetically encoded fluorescent redox sensors. *Biochimica et Biophysica Acta*. **1840** (2), 745–756 (2014).
- 20 Nietzel, T. *et al.* Redox-mediated kick-start of mitochondrial energy metabolism drives resource-efficient seed germination. *Proceedings of the National Academy of Sciences of the United States of America*. **117** (1), 741–751 (2020).
- 21 Albrecht, S. C. *et al.* Redesign of genetically encoded biosensors for monitoring mitochondrial redox status in a broad range of model eukaryotes. *Journal of Biomolecular Screening*. **19** (3), 379–386 (2014).
- 22 Albrecht, S. C., Barata, A. G., Grosshans, J., Teleman, A. A., Dick, T. P. In vivo mapping of hydrogen peroxide and oxidized glutathione reveals chemical and regional specificity of redox homeostasis. *Cell Metabolism*. **14** (6), 819–829 (2011).
- 23 Breckwoldt, M. O. *et al.* Multiparametric optical analysis of mitochondrial redox signals during neuronal physiology and pathology in vivo. *Nature Medicine*. **20** (5), 555–560 (2014).
- 24 Ricke, K. M. *et al.* Mitochondrial dysfunction combined with high calcium load leads to impaired antioxidant defense underlying the selective loss of nigral dopaminergic neurons. *Journal of Neuroscience*. **40** (9), 1975–1986 (2020).
- 25 Bjornberg, O., Ostergaard, H., Winther, J. R. Mechanistic insight provided by glutaredoxin within a fusion to redox-sensitive yellow fluorescent protein. *Biochemistry*. **45** (7), 2362–2371 (2006).
- 26 Shokhina, A. G. *et al.* Red fluorescent redox-sensitive biosensor Grx1-roCherry. *Redox Biology*. **21**, 101071 (2019).



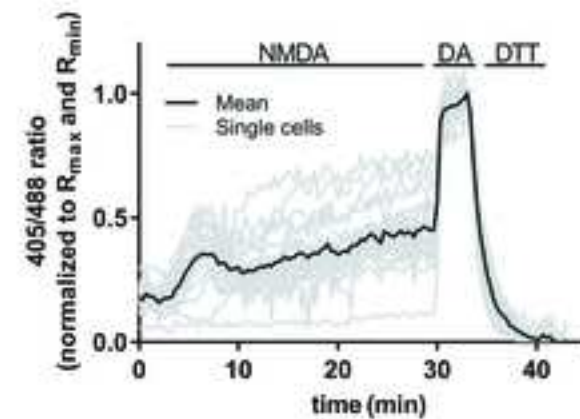




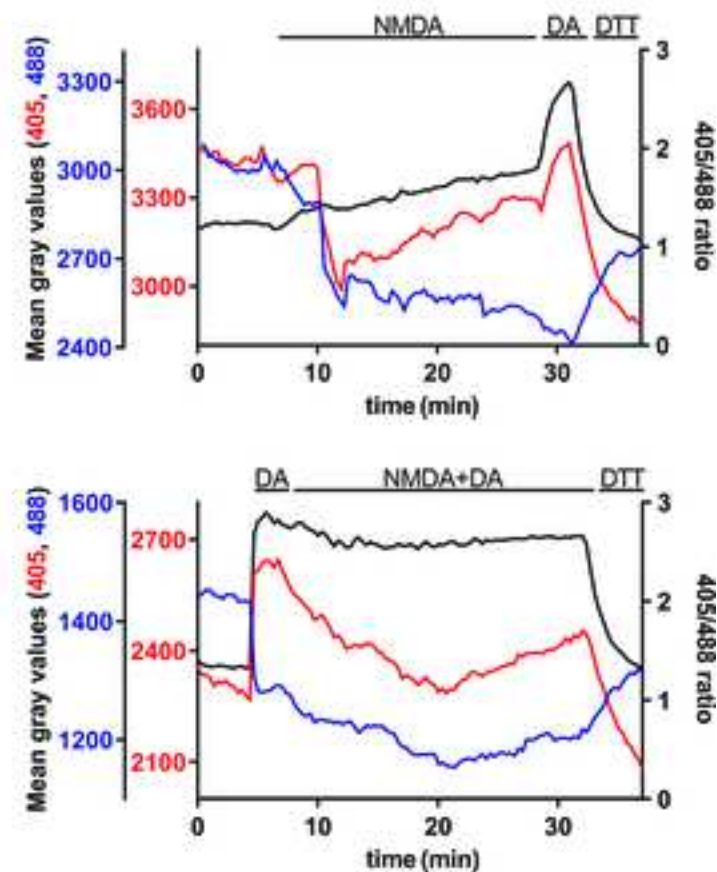
A



B



C



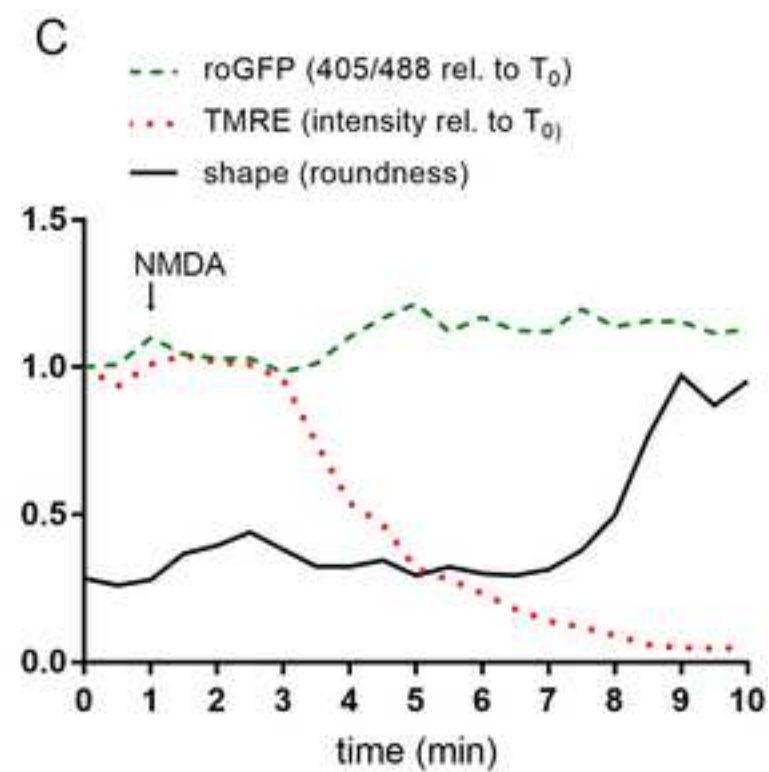
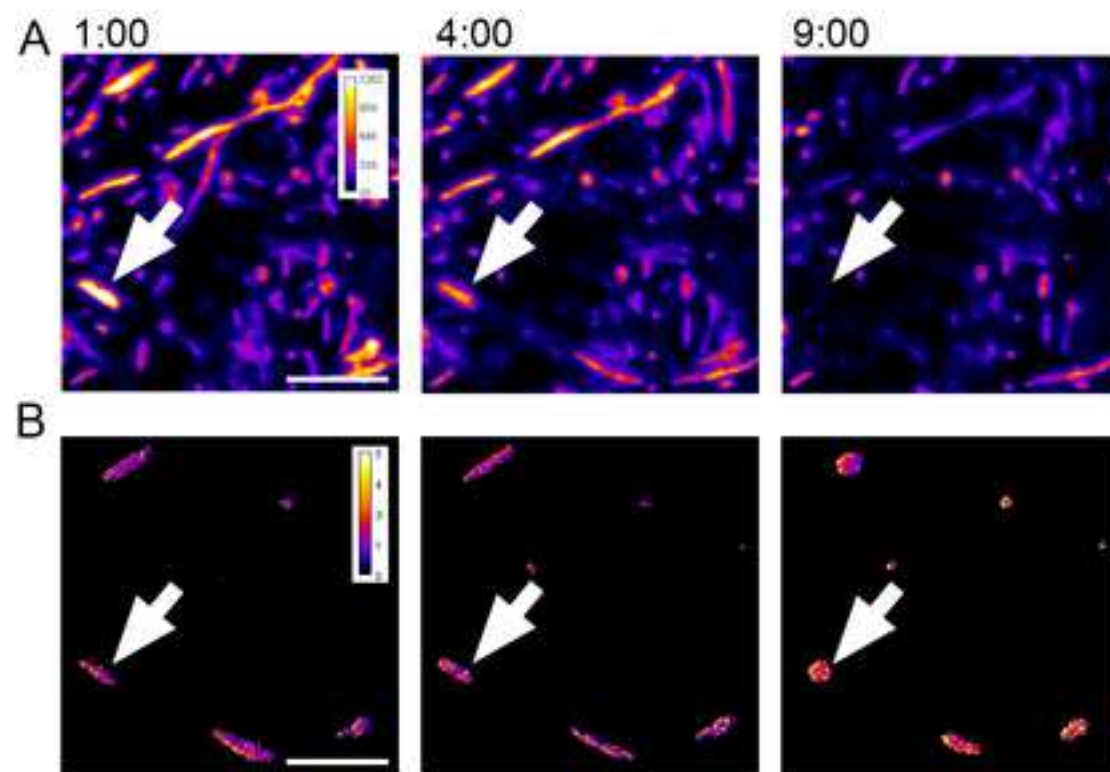


Table 1

Component	MW	Concentration (M)	Amount (g)	Volume (mL)
NaCl	58.44	5	14.61	50
KCl	74.55	3	1.12	5
MgCl ₂ ·6H ₂ O	203.3	1.9	2	5
CaCl ₂ ·2H ₂ O	147.01	1	1.47	10
Glycine	75.07	0.1	0.375	50
Sucrose	342.3	1.5	25.67	50
Sodium pyruvate	110.04	0.1	0.55	50
HEPES	238.3	1	11.9	50
Glucose	180.15	2.5	45	100

Table 2.

Component	Stock solution (M)	Final concentration (mM)	Volume (mL)
NaCl	5	114	2.3
KCl	3	5.29	0.176
MgCl ₂	1.9	1	0.053
CaCl ₂	1	2	0.2
Glycine	0.1	0.005	0.005
Sucrose	1.5	52	3.5
Sodium pyruvate	0.1	0.5	0.5
HEPES	1	10	1
Glucose	2.5	5	0.2



Click here to access/download

Table of Materials

Materials_R1.xls



Dr. Carlos Bas-Orth
Institute for Anatomy and Cell Biology
Dept. of Medical Cell Biology
University of Heidelberg
Im Neuenheimer Feld 307
69120 Heidelberg
Germany

Nilanjana Saha, PhD
Review Editor
JoVE
nilanjana.saha@jove.com

RE: Manuscript JoVE63073

Dear Dr. Saha,

We would like to thank you and the reviewers for the careful and very detailed review of our manuscript. We appreciate your insightful comments that we think helped to improve the manuscript. As per your and the reviewers' suggestions, we made several additions and changes to the text, figure legends and figures, to make the protocol easier to follow and implement by a wide range of interested readers. Please see below for a detailed point-by-point response to the individual comments.

We hope that the manuscript is now acceptable for publication in the Journal of Visualized Experiments and we look forward to recording the associated video part.

With kind regards,



Carlos Bas Orth

Point-by-point response to editorial and reviewers' comments:

Editorial comments:

Changes to be made by the Author(s):

1. Please take this opportunity to thoroughly proofread the manuscript to ensure that there are no spelling or grammar issues.

We carefully proofread the manuscript.

2. Please try to make the Title a little more concise. For example, “Live Imaging of the Mitochondrial Glutathione Redox State in Primary Rat Cortical Neurons using a Ratiometric Indicator”.

We changed the title accordingly.

3. Please rephrase the Summary to clearly describe the protocol and its applications in complete sentences between 10-50 words: “The present protocol describes. ...”. Here the word limit is exceeding.

We rephrased the summary to adhere to the word limit.

4. Please revise the text to avoid the use of any personal pronouns (e.g., "we", "you", "our" etc.).

We revised the text to avoid use of personal pronouns as much as possible.

5. Please ensure that abbreviations are defined at first usage.

We double-checked that abbreviations are defined at first usage.

6. JoVE cannot publish manuscripts containing commercial language. This includes trademark symbols (™), registered symbols (®), and company names before an instrument or reagent. Please remove all commercial language from your manuscript and use generic terms instead. All commercial products should be sufficiently referenced in the Table of Materials (including reagents, instruments, software, etc.). Please sort the Materials Table alphabetically by the name of the material.

For example, Sigma-Aldrich, Carl Roth, Parafilm, Falcon, Fiji, Leica, Nikon, Hamamatsu, TokaiHit, ImageJ, etc.

Company names before instruments have been removed. They are now mentioned in the materials list.

7. Introduction: Please support the statements of Paragraph 1 with more published References.

We now included additional references.

8. Please note that your protocol will be used to generate the script for the video and must contain everything that you would like shown in the video. Please ensure you answer the “how” question, i.e., how is the step performed? Alternatively, add references to published material specifying how to perform the protocol action. There should be enough detail in each step to supplement the actions seen in the video so that viewers can easily replicate the protocol.

We double-checked the protocol and we are confident that it includes sufficient detail to allow readers to easily replicate the protocol.

9. Please add more details to your protocol steps:

Line 119/131: How long these solutions can be stored?

Line 140: Please specify how the mixing is done.

Line 145: Please specify on what basis the sucrose concentration should be modulated.

We now added the requested details. We are confident that a scientist with a basic laboratory training will be able to calculate and measure osmolarity.

10. Please include one-line space between each protocol step and then highlight in yellow up to 3 pages of the Protocol (including headings and spacing) that identifies the essential steps of the protocol for the video, i.e., the steps that should be visualized to tell the most cohesive story of the Protocol. Remember that non-highlighted Protocol steps will remain in the manuscript, and therefore will still be available to the reader.

Individual steps of the protocol were separated by one-line spaces and the steps that should be visualized in the video had been highlighted in yellow in the submitted manuscript already. We are not exactly sure what we should change here. Please specify.

11. Please ensure that the highlighted steps form a cohesive narrative with a logical flow from one highlighted step to the next and is in line with the Title of the manuscript. Please highlight complete sentences (not parts of sentences). Please ensure that the highlighted part of the step includes at least one action that is written in the imperative tense.

The highlighted steps conform with these guidelines.

12. Please provide reprint permissions for the reuse of the Figures.

The figures are from one of our own publications in the journal *Antioxidants and Redox Signaling* which grants authors the right to reuse figures and text without the need to obtain a specific permission, and from an article published with open access under a Creative Commons CC-BY license that allows reuse of the material without the requirement of obtaining permission from the publisher. Therefore, we cannot obtain reprint permission from the publishers. Instead, we uploaded screenshots from the respective permission request websites.

13. Discussion: Please support the statements of Paragraph 1 with more published References.

We now added more references to support our statements.

14. Figure 5C: Please provide the y-axis description.

The y-axis description is different for each of the three traces depicting three different modalities. For clarity and readability, we added a description to the figure caption, rather than adding three labels to the axis in the figure. Please let us know if you agree.

15. Please spell out the journal titles in the References.

As discussed, this will be done by the editorial office. Thank you for your support.

Reviewers' comments:

Reviewer #1:

Manuscript Summary:

Oxidative stress is implicated in normal aging and is a major contributor to cell damage and death in most neurodegenerative diseases. Oxidative stress can result from increased reactive oxygen species production, decreased antioxidant levels/activity or combinations of both. The

mechanisms by which reactive oxygen species imbalances occur are largely unknown, and they may vary with disease pathology. Thus, there is a tremendous need for methods that facilitate identification of oxidative stress sources and methods to moderate efficacy of antioxidant strategies. Mitochondria are major reactive oxygen species producers; accordingly, they have relatively high levels of antioxidants. They are also the gatekeepers of intrinsic apoptosis, which is triggered when oxidative stress becomes insurmountable. The authors present a powerful and elegant method for characterizing the contribution of mitochondrial glutathione activity, which can be observed along with mitochondrial morphology and membrane potential in living neurons. This method allows the researcher to track the progression of mitochondrial stress and the effects of intervention in real time. This protocol is suitable for characterizing steady-state glutathione redox status as well as for observations of drug application therapies for disease models. Thank you for your kind evaluation of our manuscript. We are glad to see that our protocol is considered highly relevant and useful by an independent expert.

Major Concerns:

Section 6.1.6. Manually adjusting the threshold will affect results. Is it possible for the experimenter to always use "Auto" or use a manually established threshold that can be applied to all images?

We agree that manually adjusting the threshold will in principle affect the results. In our hands, however, the 405:488 nm ratio is remarkably robust to moderate changes in lower and upper threshold settings used to select pixels for analysis. To reduce any potential bias introduced by the observer, we agree that using the same method for all images is important. Because using a manually established global threshold for all images can often be problematic (e.g. due to image-to-image variation in uneven illumination or background intensities), an automated threshold determination is highly preferred (see for example: <https://petebankhead.gitbooks.io/imagej-intro/content/chapters/thresholding/thresholding.html>)

We now included a note in step 6.1.6. to provide further guidance for the readers.

Minor Concerns:

- Confirm copyright use for previously published data.

We had confirmed permission before using published data in our manuscript and we now mention this in the figure legends. In fact, one published figure is from one of our own publications and can be re-used by us in line with our author copyright agreement. The data in Hansen 2004 was published as open access under a creative commons license which permits re-use as long as the original source is cited.

- It is unclear from where in Hansen et al., 2004 the data in figure 1B come. Specify the figure from which the data came, and explain how the original data were modified to create figure 1B. Are fluorescence emissions similar for roGFP1 (Hansen et al.) and roGFP2 (here)?

The data were drawn based on figure 1B in Hansen 2004. We now added this information to the figure legend. Figure 1B in Hansen 2004 shows roGFP2 emissions, whereas Figure 1A in Hansen 2004 shows roGFP1 emissions.

- Add citation for source that reports mitochondrial GSH concentrations (lines 59-60).

We now added the citation for the 1-5 mM GSH concentrations. In addition, we performed an additional literature search and found publications that provide estimates of up to 15 mM GSH in mitochondria. We now cite an additional publication and we changed the concentration range to 1-15 mM accordingly.

- Section 2. Indicate at what temperature this procedure should be carried out.

TMRE is added to the cells under a tissue culture laminar flow hood (we now added this information) and then are placed back into the incubator for dye loading. Therefore, loading occurs at 37°C, but we don't think it is necessary to mention that a cell culture incubator for primary neurons should be set to 37°C.

- Section 3. Indicate temperature at which this step should be carried out.

Similar to electrophysiological recordings or calcium imaging, experiments with roGFP can be performed at room temperature or at 35-37°C. The sensor itself works under both conditions, but obviously cell biology (enzyme and signaling kinetics, mitochondrial motility and dynamics, neuronal activity) will differ. It is up to the user to decide between technically more simple imaging at room temperature or physiologically more relevant imaging at 37°C.

We now added a note to section 3 to point this out.

Should the user perform optimization steps before each experiment?

This is not necessary. Once the microscope settings have been optimized for an experimental setting involving a certain microscope and a certain method for expression, the same settings can typically be used for subsequent experiments. We now added this information to the text.

Should the user expect detectable differences in transfection efficiency between experiments?

In our opinion, this strongly depends on the method of gene transfer (lipofection, calcium phosphate transfection, viral gene transfer) and the experience of the researcher in handling primary neurons and performing gene transfer. In our hands, an experienced researcher using an established transfection or infection protocol typically obtains comparable efficiency between experiments. However, given the above mentioned considerations, we cannot provide a generalized statement here.

Would varying transfection efficiencies affect reproducibility?

As long as a sufficient number of cells is transfected and can be imaged per experiment, varying transfection efficiencies should not affect reproducibility. This might, however, depend on the specific context of the users' experiments. Therefore, we prefer to not give a general statement.

- Section 3.9. Explain how the user is to determine signal-to-noise ratio. If this information is not provided by the imaging system, can the user calculate it?

We now added instructions on how to calculate the signal-to-noise ratio.

Also, are the target signal intensities for each fluorophore average intensities for the entire image? Please clarify.

The target signal intensities are average intensities within single-cell or single-mitochondria ROIs. We now added this information to the text.

- Section 3.14. Indicate what values in the data table represent the 405:488 ratio.

We are not sure what is meant by data table in this context. As described in section 6, the user will create a 405:488 ratio image and measure the ratio in individual ROIs. These values represent the 405:488 ratio. The values will be exported to a spreadsheet software and it is up to the user how they organize their spreadsheet.

- Section 6.2.2. It appears that results should be exported before measuring ROIs in the thresholded 405 and 488 nm images. Data disappear when new measurements are taken. Whether data are deleted from the results window or new measurements are added below existing data depends on the settings selected in FIJI. Nevertheless, to make sure new users don't lose their data, we now added an "export data" step after each measurement.

- Section 6.2.3 and 4. Explain how the same ROIs can be added to the thresholded 405 and 488 nm images.

When following the protocol and using the procedure described in step 6.2.2 (ROI Manager | ctrl+A to select all ROIs | More | Multi Measure), the same ROIs from the ROI manager will automatically applied to the 405 and 488 nm images. We now added a note to specify this.

- Section 6.2.7. Provide step-by-step instructions on how to generate XY-graphs for 405 and 488 nm traces. Explain how to interpret the graphs to verify that there is no bleaching, etc.

The term XY-graph may be misleading (readers might think it involves plotting 405 vs 488 nm intensities). We apologize for this and now rephrased the instruction to: "Generate intensity vs time plots of the 405 and 488 nm traces."

We also added an example to explain what we mean with "traces move into opposite directions".

- It would be helpful if authors provided steps for measuring mitochondrial morphology using roGFP.

We now describe steps for measuring morphology in parallel to roGFP intensity (see new section 6.4).

- Figure 3B,C and line 413. The graphs do not convince the reader that there is a statistically significant difference between conditions.

We agree that the conditions are not statistically different, and in the manuscript we don't claim they are. Moreover, as detailed in the figure legend, the data are based on three replicate coverslips per condition from one preparation of primary neurons. To make any meaningful claims about statistics, the experiment would have to be repeated several times with cells from independent neuronal preparations. However, the aim of this figure and, in fact, the whole article, is not to present new scientific findings, but is instead to provide a protocol of how to perform a specific method and to present typical results that can be obtained in an experiment. As described in the text and legend, in this example of quantifying basal redox states under different conditions, we simply show that in this specific experiment after data normalization a subgroup of oxidized cells can be identified in one of the conditions.

- Lines 509-510. Are Grx1-roGFP2 constructs targeted to to presynaptic terminals or dendritic spines commercially available? If so, from where?

We are not aware of commercially available constructs. However, they can be generated by standard molecular biology techniques.

Reviewer #2:

Manuscript Summary:

Authors detail in this manuscript the ability and use of Grx1-roGFP2 to measure redox changes related to GSH/GSSG variations. Experimental and analysis details are provided, to facilitate both the performance of experimental acquisitions and the processing of images and data

analysis. It is relevant that authors do highlight several details to be considered, such as the influence of pH or the need to calibrate the sensor and check redox detection limits, a feature that is not always included in analyses performed with sensors as the ones. Below, some comments intend to implement several considerations:

Thank you for your kind evaluation of our manuscript. Please find below our answers to your specific queries.

Major Concerns:

1. Please elaborate on key features of Grx1-roGFP2 as a tool, i.e. dynamic range, bleaching, stability, etc. Other similar probes should be also better referred to measure general redox status and GSH/GSSG pair. Alternatives such as the close similar Grx1-roCherry (Shokhina et al., 2019) should be briefly referred and compared. It is relevant to discuss and highlight that procedures described in this manuscript may be extended with little changes to the use of other probes.

We agree that information on biophysical properties of a sensor are important for evaluating its performance and limitations. As we understand, however, the aim of this article is to specifically present a detailed but concise protocol on how to perform Grx1-roGFP2 live imaging in cultured neurons. It is not supposed to be a review about roGFP. For biophysical details of the sensor, the interested reader is referred to a number of excellent articles by the developers of the sensor that are cited in the manuscript. Likewise, we think the article should not be a general review of fluorescent redox sensors. Several excellent reviews on that topic are available in the literature and we do cite one in the revised manuscript. We do not have practical experience with Grx1-roCherry or rxYFP-Grx1p, and therefore are not in a position to evaluate the performance of these sensors. We agree, however, that it is helpful to make the readers aware of spectral variants. Therefore, we now mention them in the discussion and cite relevant articles for further reading.

2. As two-photon in vivo intra-vital microscopy is not always available to several labs, is it possible to use Grx1-roGFP2 to measure samples ex vivo; i.e. brain slices? What considerations should be taken in such case for manipulations and to avoid redox alterations?

It is possible to measure Grx1-roGFP ex vivo, e.g. in brain slices or muscle explants. We now explicitly mention this possibility in the discussion. Preparation of acute brain slices or tissue explants is a delicate procedure with several critical steps. An accurate description of these methods therefore is beyond the scope of this article. The interested reader may find relevant information in the cited references.

3. Since an active Grx1 is overexpressed in the cell, this may change the endogenous redox levels. Thus, resting levels may be biased by Grx1 overexpression and even transfection efficiency, even if ratiometric or normalized by max/min fluorescence. May Grx1-roGFP2 be more convenient to monitor acute changes once in equilibrium (fold increases/decreases), after stimulating ROS production with a certain challenge?.

We agree that, in general, introduction of a biosensor might affect the kinetics of the reactions to be measured. For example, it is well known that calcium indicators are also calcium buffers that will affect calcium kinetics above a certain concentration of indicator. In the case of Grx1, we don't think that it will change resting redox levels, because Grx1 itself is not quantitatively involved in reducing oxidized substrates. Instead, its function is to catalyze GSH-dependent reduction of substrates. Overexpression of Grx1 might therefore increase the speed of substrate/GSH equilibration, i.e. equilibrium might be reached faster, but it should not change the equilibrium itself. In fact, these increased kinetics are the major advantage of Grx1-roGFP2 and

also rxYFP-Grx1p as compared to roGFP2 or rxYFP, because it ensures that any cellular changes in the GSH/GSSG ratio are rapidly and reversibly mirrored by changes in the roGFP(reduced)/roGFP(oxidized) ratio and can thus be visualized in real time as they occur in the cells.

4. Settings and considerations should be extended to TMRE. Set up experiments must check a base line, with no drops in TMRE by bleaching, phototoxicity or altered mitochondrial function. Addition of cyclosporine H (usually 1 μ M) does not affect mitochondrial function and may be useful to avoid membrane potential-independent TMRE leakage. Even if indicated, please remark that TMRE must be always present and equilibrated. Addition of a mitochondrial uncoupler (i.e. 1-2 μ M FCCP) will help calibrating fluorescence at the end of experiments.

We agree that settings for TMRE imaging need to be optimized as well. The same holds true for any other indicator that will be used in combination with roGFP imaging. Because the focus of this article is on mitochondrial Grx1-roGFP and we can't know which other additional indicators will be used by the readers, we prefer not to provide detailed instructions on other specific indicators such as TMRE. We now, however, added a note to section 3 that points out the need for optimization of imaging parameters for additional indicators. We are confident that a trained researcher who masters roGFP imaging on their setup will be able to independently optimize settings for their additional indicators of choice, including TMRE. Moreover, a rich literature on TMRE imaging exists that will guide the users along that way.

Inclusion of TMRE in the imaging buffer and stimulation solutions was described in step 2.5. As per this reviewer's suggestion, we now rephrased the instructions to make an even stronger statement.

5. Under this reviewer's experience, it may not be necessary 60 min incubation to reach TMRE equilibrium, and this time could be reduced by half the time, always conditioned to confirmation of TMRE persistence in mitochondria during the experiment.

We agree that less than 60 minutes may be sufficient to reach TMRE equilibrium under some circumstances. However, we obtained more robust results (i.e., less coverslip-to-coverslip and cell-to-cell variability) when pre-incubating for at least 60 minutes as compared to 30 minutes. In addition, 60-minute equilibration time is recommended in several methods articles (see for example Brand and Nichols 2011 Biochem. J. 435). We therefore prefer to recommend 60 min incubation. It is of course up to the reader to test and validate different incubation times.

6. When processing in Fiji, could Autoscale or Threshold alter pixel intensity or normalization, thus affecting comparisons between images from different chambers (even if later normalized by calibrations)? Please discuss this in the main text.

Autoscale in Fiji affects how data is displayed on the computer screen, but it does not affect pixel intensity. Since images are recorded at 12 to 16 bit, but intensities are typically below 5000, without autoscaling the image would look very dark on the screen and it would be difficult to visualize cells. We now added a note to section 6.1.1 to inform readers about this function.

Threshold is used to select which pixels will be analyzed and which pixels are considered background. It does not alter pixel intensities. In general, automated threshold detection is preferred over manual selection of individual thresholds and is also preferred over the use of a global threshold (see for example: <https://petebankhead.gitbooks.io/imagej-intro/content/chapters/thresholding/thresholding.html>).

We now added more information about selection of automated threshold determination methods to step 6.1.6. to provide further guidance for the readers.

7. Changes in Fig. 1 are subtle. Do authors have evidence for major changes in redox status upon addition of H₂O₂, NAC or other antioxidants, or GSH alterations (i.e. with L-BSO) that may implement the figures?

Fig.1 shows the excitation spectra of fully reduced and fully oxidized roGFP2. This reviewer is probably referring to a different figure. Please specify. In general, Grx1-roGFP2 has been used to detect redox changes upon H₂O₂ treatment in different cell types (including primary neurons in our previous publication by Depp et al. that is cited in the manuscript), in different publications from different research groups.

8. TMRE fluorescence and mt-GPx1-roGFP2 fluorescence is not fully paralleled in Fig. 5a, thus losing mitochondria in mt-GPx1-roGFP2 images. This may indicate that manipulations of fluorescence for normalization or ratio are excluding the visualization of some mitochondria. Since it is predicted that all mitochondria (even if depolarized) import the redox sensors, raw micrographs illustrating the real distribution of mt-GPx1-roGFP2 are critical to validate it as a global sensor for the whole mitochondrial network.

The reviewer is correct with the observation that not all TMRE-positive mitochondria do express mito-Grx1-roGFP2. This is, however, not due to image processing or normalization. It is due to the fact that the efficiency of AAV-mediated gene transfer is less than 100%, typically around 70-90%, sometimes less. Therefore, only a subpopulation of neurons contains roGFP-labelled mitochondria, whereas all neurons take up the small molecule dye TMRE and thus contain TMRE-labelled mitochondria. Within a single roGFP-positive neuron, typically all mitochondria are co-labelled with TMRE and roGFP. The distribution of roGFP-positive mitochondria in the ratio images is the same as in the individual 405 nm excitation and 488 nm excitation channels. To clarify this point, we added a note to the figure legend.

9. Treatments other than NMDA could induce acidification, as referred. How could mt-GPx1-roGFP2 measurements be solved under excessive acidification?

As discussed in the article, while the 405/488 nm ratio is not affected by acidification, the generally weak 405 nm-excited signal can drop below detection limit upon acidification. We are not aware of any measures to solve this problem. This is why we mention this issue as a major limitation of the sensor.

Minor Concerns:

1. Line 58: Should it be instead?: '... and ultimately mitochondrial and cell viability'

The sentence was meant to say that redox potential affects mitochondrial viability, which ultimately affects cellular viability. We now rephrased the sentence to avoid misunderstanding.

2. Line 80: Please detail what mixed 1/2 serotype is referred.

We now described the serotype more accurately and provided an additional reference.

3. Even if they can be purchased, amounts to prepare sodium pyruvate, HEPES and glucose master solutions should be included in Table 1.

We now added this information to Table 1 and included the source for the respective powder reagents in the Materials list.

4. Is it relevant the volume of aliquots for long-term storage? In case relevant, please indicate why the shown volumes are recommended (i.e. maximum amount needed per X wells or similar). The volumes of aliquots were based on the volumes needed in our typical experiments. This is likely to be different for different sets of experiments (depending on how many coverslips are imaged per day, which drugs are being added, etc.). We therefore now removed the recommended volumes.

5. Even more important than sealing with parafilm, TMRE should be protected from light. Thank you for pointing out this important aspect. We fully agree and now added this information to the protocol.

6. Please indicate in Table 2 the volume of H₂O to be added and the final volume of the imaging solution. pH of the final solution should be indicated, as it may be highly relevant besides osmolarity.

The final volume of imaging buffer is specified in step 1.3.1 that describes how to prepare the buffer. For clarity, we now also added this information to Table 2. We also added the desired pH of the final solution.

7. It may be somehow confusing that NMDA stock solutions could be stored and then it is indicated that fresh solutions should be prepared. May it be more convenient to refer this note to imaging buffer instead (and then add NMDA or other frozen aliquots)?

Thank you for pointing this out. The sentence might indeed be misleading. It was meant to say that stimulation solutions containing diluted drugs should be prepared fresh by adding the concentrated drugs just before the experiment. We now rephrased the sentence accordingly.

8. DTT is unstable in solution and may be oxidized after 3 months at -20°C, thus losing activity. Due to its relevance for calibration, may it be more convenient to prepare fresh solutions or remark stability.

We agree with this important point and we now point out limited stability in the protocol. Since an excess of DTT is added to the cells, a minor loss of activity during few weeks' storage at -20°C does not affect calibration in our hands. We therefore do not think it is necessary to prepare fresh DTT for every experiment in this case.

9. When read before the main text, in epigraph 1.4 is hard to interpret the addition of solutions and final volumes or concentrations ... A solution could be to place 1.4.3 at the place of 1.4.2. Indicate that additions are sequential as follows, and state that DTT is added in the final step, after retiring the whole volume in the chamber.

Thank you for pointing out this limitation. We now added a note to section 1.4 (right before 1.4.1) to make the reader aware of the basic stimulation scheme. We also added the information that DTT is added after aspirating the buffer from the chamber.

10. To be consistent, volumes of imaging buffer should be 6.986 mL for epigraph 1.4.2 and 6.972 mL for 1.4.3.

You are right. We changed the text accordingly.

11. For the naïve readers, please briefly explain what TMRE in non-quench mode is.

Because this protocol focuses on roGFP imaging, and because more than 60 editorial and

reviewer queries need to be included during this revision, we prefer not to further increase the volume of this article with additional explanations of basic concepts. Instead, we cite an excellent reference that very elegantly describes the theoretical and technical aspects of mitochondrial membrane potential imaging for the interested reader.

12. Epigraph 2.5: 'add 20 nM TMRE to imaging buffer' should be 'add TMRE to get final 20 nM in imaging buffer'

We agree that this instruction was not fully accurate. We now rephrased the sentence.

13. It is recommended to emphasize that ROIs should include only regions with fluorescence and avoid including the surroundings of the cell or nuclei. It is also to be considered that ROIs cannot remain empty upon cellular displacement.

Because background pixels are defined as Not a Number (NaN) during threshold application (step 6.1.6), they are not considered during measurement of pixel intensities within a ROI. Therefore, including surrounding background pixels in the ROI does not affect the measurement. If cells move during time lapse imaging due to drift of the chamber (this is probably meant by cellular displacement), we recommend to perform image registration before analysis.

14. Please assign oxidation and reduction in the color-coded scales.

We now added this information to the figure legends.

A consistency in the labelling of y-axis is missing; Fig. 4B labeling is right and may be extended to other graphs (suggestion: you can use '405/408 nm ratio fluorescence' should not normalized). We agree that labelling differs between figures, but we respectfully disagree that only 4B is right. In fact, there are different valid ways to label the graphs. '405/408 nm ratio fluorescence', in contrast, is not correct. This should rather be '405/488 nm fluorescence ratio'. To improve consistency, we re-labelled axes in Fig. 3 to '405/488 ratio' and 'normalized 405/488 ratio'.

15. The main text should better explain differences between Fig. 3b and c analysis and results, as well be specifically referred in the main text.

We agree that it would be helpful to better point out the different analyses and results, which will underscore why normalization is an important step. We now discuss this in the main text in more detail.

State in the text whether differences reached statistical significance.

As mentioned in the figure legend, the data in this experiment are from three replicate coverslips per condition from one primary neuron preparation. To make any meaningful claims about statistics, this experiment would need to be repeated several times with neurons from independent preparations. The figure is, however, not meant to present novel scientific findings but rather illustrates a typical experimental outcome of the method and illustrates the difference between raw and normalized ratios.

16. While it is explained in Fig. 4C legend, the text does not clearly refer how pH and redox signaling were dissected. Please extend it briefly in the main text.

In the results section, we now explain in more detail the principle of this control experiment.

17. Include other ratiometric, genetically-encoded probes in the discussion, as suggested in the main comments to this manuscript.

We now included other ratiometric genetically-encoded redox probes in the discussion.

18. Line 524: Are there evidence for the accuracy and validation of mt-GPx1-roGFP2 quantification in isolated mitochondria? Along with the usage of mitochondrial specific inhibitors, a good alternative to mitochondrial isolation (which may damage mitochondria and alter redox balance and GSH equilibrium) would be the permeabilization of cells (i.e. with digitonin) to facilitate a direct access to mitochondria still in the cell.

Please refer to the cited publication for information on validation of roGFP2 quantification in isolated mitochondria. Again, this article is not meant to be a comprehensive review about imaging of roGFP and potentially many other indicators in a variety of cells and organisms. It is required (by the journal guidelines) to be a concise description of a specific method, which in our case is mitochondrial roGFP imaging in primary neurons.

We also are certainly aware of the possibility to use digitonin for the study of mitochondria in permeabilized cells. Again, an extensive discussion of these aspects is, unfortunately, beyond the scope of this article.

Reviewer #3:

Manuscript Summary:

The authors provide systematic description of the methodology to detect glutathione redox state for live cell imaging and compatability with other methodologies using a glutathione sensitive fluorescent construct. This is an important tool as changes in metabolic and redox states have been shown to be a major contributor in many neuro-degenerative disease states, such as Alzheimer's disease, Parkinsons, etc. The manuscript is well written and easy to follow.

Thank you for your kind evaluation of our manuscript. We are glad that the protocol is easy to follow by an independent reader.

Minor Concerns:

Line 445 - the concentration of NMDA was increased to 60 uM for the experiments with TMRE, when previous experiments only used 30 uM. The rationale for this is unclear.

We and others typically use NMDA concentrations between 20 and 100 uM to induce excitotoxicity in primary neurons. Sensitivity to NMDA partially depends on cell type (cortical vs hippocampal), culture conditions (especially media composition), basal activity level, and age of the neurons. The example experiment shown in figure 5 was part of an ongoing series of experiments in which we were using 60 uM NMDA in rat cortical neurons, while the experiments in figure 4 are from a previous study (Depp et al. 2018) with mouse hippocampal neurons in which we used 30 uM NMDA. In general, we would expect similar results in the TMRE experiments when using 30 uM NMDA, but due to limited time and availability of primary neurons, we decided not to perform additional experiments for this figure but instead use recently generated data from the lab.

Line 555 - please provide reference for the experiments on retinal flatmounts with roGFP in the discussion

Since we were not able to obtain reliable measurements of roGFP ratios in live retina, we did not publish any data from these experiments. We now added 'Depp and Bas-Orth, unpublished observation' as a reference.

Images of neurons are not very clear - a DIC image to show neuronal structure would have provided better clarity. The location of the fluorescence within the neuron is not specified, whether cell body, dendrite, axon, etc, since mitochondria in neurons are concentrated in the terminals. Also are there regional differences in redox state within the neuron based on this construct?

Whereas synaptic terminals certainly contain a high density of mitochondria, synaptic terminals are small structures and, therefore, do not contain the majority of neuronal mitochondria. In cultured primary neurons, the soma is densely packed with mitochondria that can hardly be optically separated even at high resolution, whereas dendrites and axons contain numerous, but more spaced out and more elongated mitochondria. Accordingly, under low magnification, mito-roGFP signal is typically detected in soma and large proximal dendrites, while at high magnification dendritic and axonal mitochondria can easily be detected.

We now added more information to figure legends 4 and 5, describing the location of roGFP signal.

In our previous publication (Depp et al. 2018, Figure 3E) we found a higher basal oxidation of dendritic mitochondria vs somatic mitochondria.

Please address stability of construct/expression for in vivo analyses, and long-term experiments, if this is a limitation for the usage of the construct.

As mentioned in the introduction, roGFP expression in primary neurons upon AAV-mediated gene transfer is stable for at least two weeks. In our hands it is stable for the entire lifetime of the primary neurons. AAV-mediated expression of fluorescent proteins in vivo is well-known to be stable for months. Besides, most in vivo studies use transgenic animals with a genomic integration of the expression construct, so we are not exactly sure, why stability of expression should be a limitation.

Reviewer #4:

Manuscript Summary:

This is a well written methods paper describing the measurement of the mitochondrial redox status by analysing the oxidation/reduction state of the glutathione system using a modified GFP as a sensor and simultaneously measuring the mitochondrial membrane potential by a small fluorescent molecule.

Thank you for your kind evaluation of our manuscript.

Major Concerns:

The novelty of this review is the simultaneous measurement of the mitochondrial redox status and the membrane potential, and the method may become even more interesting when ex vivo studies can be done on brain slices instead of cultivated cells. Measurements of the mitoRO-GFP signal and also the measurement of the mitochondrial membrane potential using TMRE have been described before in JoVE.

We agree that ex vivo imaging would be interesting to many readers. We personally do not have extensive experience with slice imaging of roGFP and, therefore, are not in a position to provide expert advice on that particular application. We do, however, cite publications that use ex vivo imaging, so that the interested reader may find further guidance.

We also are aware that roGFP and TMRE imaging have been described before in JoVE. To our knowledge, a detailed protocol for use of mito-Grx1-roGFP2 is not yet available. By adding

specific instructions for performing these experiments in neurons, on how to optimize microscope settings, on how to perform min/max normalization of the sensor, and on how to combine this with morphological quantification (added during revision), we hope to provide useful information that is not contained in previous JoVE articles.

Minor Concerns:

Some minor comments:

- In the title, it should say "primary neurons", since both cortical and hippocampal neurons are used later.

Thank you for pointing this out. We changed the title accordingly.

- P. 6, line 113, 117 and 121, 127: Please describe shortly already here why you use these substances, i.e. what are they doing ?

We now added this information, so it will hopefully be clearer to readers at first glance.

- P. 24, line 5 - 9: Here, a recent study by Ricke et al., J Neurosci 26 (2020) should also be quoted.

We are not exactly sure to which section the reviewer is referring, because in the version available to us, p.24 l. 5-9 is about the advantages of roGFP over chemical dyes. We can imagine that the comment refers to the possibility of roGFP2 2P imaging in tissue explants. We now cite this reference at the corresponding position in the revised manuscript.



RightsLink®



Home



Help



Live Chat



Sign in



Create Account



Synaptic Activity Protects Neurons Against Calcium-Mediated Oxidation and Contraction of Mitochondria During Excitotoxicity

Author: Constanze Depp, Carlos Bas-Ortiz, Lisa Schroeder, et al

Publication: Antioxidants & Redox Signaling

Publisher: Mary Ann Liebert, Inc.

Date: Oct 20, 2018

Copyright © 2018, Mary Ann Liebert, Inc.

Quick Price Estimate

No content delivery.

This service provides permission for reuse only. If you do not have a copy of the article you are using, you may copy and paste the content and reuse according to the terms of your agreement.

To request a copy please contact reprints@liebertpub.com

Mary Ann Liebert, Inc. publishers does not require authors of the content being used to obtain a license for their personal reuse of full article, charts/graphs/tables or text excerpt.

I would like to... 

reuse in a journal/magazine

I will be translating... 

no

I am a/an... 

author of the requested content

Distribution quantity I would like to use... 

charts/graphs/tables

My currency is...

USD - \$

Number of charts/graphs/tables... 

2

Quick Price

Click Quick Price

My format is... 

print and electronic

QUICK PRICE

CONTINUE

To request permission for a type of use not listed, please contact reprints@liebertpub.com

Publisher: Elsevier

Copyright © 1969, Elsevier

Creative Commons

This is an open access article distributed under the terms of the [Creative Commons CC-BY](#) license, which permits unrestricted use, distribution, and reproduction in any medium, provided the original work is properly cited.

You are not required to obtain permission to reuse this article.

To request permission for a type of use not listed, please contact [Elsevier](#) Global Rights Department.

Are you the [author](#) of this Elsevier journal article?